



Amide proton transfer-weighted magnetic resonance imaging for the evaluation of testicular spermatogenic function: a preliminary study

Guanglei Tang^{1*}

Shulin Ma^{1*}

Wenhao Fu¹

Weijian Yun¹

Yang Peng¹

Jian Guan^{1,2}

¹The First Affiliated Hospital, Sun Yat-Sen University, Department of Radiology, Guangdong, China

²Linzhi People's Hospital, Department of Radiology, Tibet, China

*Joint first authors

Corresponding authors: Jian Guan, Yang Peng

E-mails: guanj6@mail.sysu.edu.cn, pengy63@mail.sysu.edu.cn

Received 23 January 2025; revision requested 21 February 2025; last revision received 17 March 2025; accepted 23 March 2025.



Epub: 20.05.2025

Publication date: xx.xx.2025

DOI: 10.4274/dir.2025.253248

PURPOSE

To determine the amide proton transfer-weighted (APT_w) imaging features in testes with age, and to assess the feasibility of APT_w magnetic resonance imaging (MRI) in assessing testicular spermatogenic function.

METHODS

A total of 23 male patients with clinically confirmed hypospermatogenesis caused by epididymo-orchitis were included in the case group (group A) and another 93 men (age range, 20–80 years) were included in the control group. The control group was divided into four subgroups: group B1 (20–34 years, n = 25), group B2 (35–49 years, n = 23), group B3 (50–64 years, n = 21), and group B4 (65–80 years, n = 24). All participants underwent 3.0T MRI scan, and the APT signal intensity (SI) and apparent diffusion coefficient (ADC) value of each testis were examined. The ADC and APT SI were independently measured by two radiologists blinded to clinical data, and average values were calculated. A power analysis was conducted to determine the required sample size.

RESULTS

APT SI was negatively correlated with age ($r = -0.510$, $P < 0.001$), whereas ADC was positively correlated with age ($r = 0.317$, $P = 0.006$). The APT SI was significantly higher in group A (1.77 ± 0.41) than in group B1 (1.43 ± 0.21), group B2 (1.37 ± 0.31), group B3 (1.30 ± 0.35), and group B4 (1.20 ± 0.35) (all $P < 0.01$). The ADC was significantly higher in group A [$(0.549 \pm 0.091) \times 10^{-3} \text{ mm}^2/\text{s}$] compared with group B1 [$(0.449 \pm 0.047) \times 10^{-3} \text{ mm}^2/\text{s}$], group B2 [$(0.475 \pm 0.022) \times 10^{-3} \text{ mm}^2/\text{s}$], and group B3 [$(0.488 \pm 0.051) \times 10^{-3} \text{ mm}^2/\text{s}$] (all $P < 0.01$), whereas no statistically significant difference was found between group A and group B4 ($P > 0.05$).

CONCLUSION

The APT SI of the normal testes decreased with age, whereas a significant elevation of APT SI was detected in patients with hypospermatogenesis caused by epididymo-orchitis.

CLINICAL SIGNIFICANCE

Hypospermatogenesis caused by degeneration or inflammation can be differentiated by APT quantity combined with ADC value.

KEYWORDS

Testis, oligospermia, orchitis, MRI, amide proton transfer

Orchitis and epididymo-orchitis are important causes of male infertility. A prolonged course of bilateral orchitis may impair spermatogenesis and lead to non-obstructive azoospermia (NOA).¹⁻³ The spermatogenic function of normal testes decreases with increasing age.⁴⁻⁶ Magnetic resonance imaging (MRI) allows for non-invasive assessment of testicular lesions and provides adequate anatomic information, satisfactory tissue contrast, and functional information.^{7,8} Functional MRI methods, including dynamic contrast-enhanced MRI,^{9,10} diffusion-weighted imaging (DWI),¹⁰⁻¹⁵ magnetization transfer imaging (MTI),¹⁶⁻¹⁸ and

MR spectroscopy (MRS),¹⁹⁻²¹ have recently provided useful additional diagnostic data for determining normal and abnormal testes.

Amide proton transfer-weighted (APT_w) imaging, a specific type of chemical exchange saturation transfer MRI, has been introduced as a novel endogenous contrast modality for MRI by detecting low concentration solutes, including mobile proteins and peptides in tissue or tumor samples with abundant amide chemical constituents.^{22,23} APT has been examined as an imaging biomarker in a variety of cancers and non-oncological diseases.²⁴⁻²⁹ Currently, a limited number of studies have evaluated APT in the assessment of human testicular metabolic profile. Whether APT_w imaging can be used to evaluate the spermatogenic potential of the testis remains unknown. The purpose of this study is to examine the APT_w imaging features of the testis with age, and to examine the feasibility of APT_w MRI in assessing testicular spermatogenic function.

Methods

Study population

The current study was approved by the Institutional Ethics Committee of the First Affiliated Hospital of Sun Yat-sen University (protocol number: 537/2022, date: 2022/11/25), and signed informed consent was obtained from all participants. The study initially included 28 consecutive men with hypospermatogenesis caused by epididymo-orchitis (age range, 22–57 years; mean age, 35 years) who underwent scrotal MRI with DWI and APT_w between June 2020 and June 2023. The inclusion criteria were as follows: (1) diagnosis of hypospermatogenesis according to the 2021 WHO guidelines³⁰ (semen analysis showing azoospermia or sperm concentration below the lower reference limit of 15 million sperm/mL of ejaculate after centrifugation in at least two tests); (2) clinical diag-

nosis of epididymo-orchitis (diagnostic criteria defined by The 2016 European guideline on the management of epididymo-orchitis³¹) based on medical history, physical examination, and laboratory tests; and (3) seminal plasma biochemistry showing elevated polymorphonuclear elastase concentration (>250 ng/mL), indicating active testicular injury by inflammation.³²⁻³⁴ The exclusion criteria included (1) poor image quality for ADC or APT_w map; (2) other testicular diseases, including testicular tumors; and (3) a history of testicular injury or surgery.

During the same period, another 111 healthy males were referred for scrotal MRI as controls. In the control group, no abnormal findings of the scrotum were found by physical examination, as well as no traumatic history of the scrotum. Volunteers under 50 years old underwent seminal plasma biochemistry and showed normal results, and those over 50 years old had genetically related children with natural insemination. The exclusion criteria were the same as described for the case group.

Among the 139 men enrolled, 15 were excluded because of APT and ADC images of insufficient quality, including motion artifacts (n = 5), poor image quality caused by B0 field inhomogeneity (n = 6), and a combination of motion artifacts and B0 field inhomogeneity (n = 4). In addition, 8 were excluded because of complications with other testis diseases or with a history of testicular injury or surgery. Among the 23 excluded cases, 5 were in the case group and 18 were controls. Thus, a total of 116 men were analyzed, including 23 men (age range, 22–57 years; mean age, 36.4 years) with hypospermatogenesis caused by epididymo-orchitis (case group A) and 93 male volunteers (control group B; age range,

20–80 years). The control group was further divided into four subgroups by age: group B1 (20–34 years, n = 25), group B2 (35–49 years, n = 23), group B3 (50–64 years, n = 21), and group B4 (65–80 years, n = 24). The study flowchart is presented in Figure 1.

Magnetic resonance examinations

All participants underwent non-enhanced MRI, DWI, and APT_w examinations in the supine position after urination using a 3.0T MR scanner (Ingenia CX, Philips Healthcare, Best, The Netherlands) with a 32-channel phased-array torso coil. Axial and coronal fast spin-echo T2-weighted imaging [repetition time/echo time (TR/TE): 2,500/65 ms] and axial spin-echo T1WI (TR/TE: 600/20 ms) images were obtained, with a small towel placed between the thighs to stabilize the testes and the penis taped to the anterior abdominal wall. An additional axial fat saturated T1W sequence was acquired when T1 hyperintense foci were detected in testes.

DWI was performed with free-breathing, with spectral attenuated inversion recovery axial single-shot spin-echo echo-planar imaging (TR/TE, 4,500/107 ms; 2 NSA) with b values of 0, 900, and 4,000 s/mm², a slice thickness of 3 mm, an intersection gap of 0.6 mm, a field of view (FOV) of 120*71 mm², a sampling resolution of 1.8*1.8*3 mm³, and a total scan time of 4 minutes and 55 seconds for each DWI scan. Moreover, APT_w imaging was performed with a three-dimensional TSE-mDixon sequence. Parameters for the APT_w sequence were as follows: saturation power, 2 μT; saturation duration, 2 s; frequency offsets, ± 3.5, ± 3.42, ± 3.58, -1,540 ppm; TR/TE, 5,864/8.8 ms; FOV, 250*346 mm²; sampling resolution, 1.8*1.8*4 mm³; slice thickness, 4 mm; sensitivity encoding factor,

Main points

- Amide proton transfer (APT) signal intensity (SI) of normal testes tended to decrease with increasing age, and apparent diffusion coefficient (ADC) of normal testes was positively correlated with age.
- Patients with hypospermatogenesis caused by epididymo-orchitis exhibited much higher APT SI compared with all age groups of controls.
- An increased APT SI combined with an elevated ADC is more likely to be associated with active or persistent inflammation.

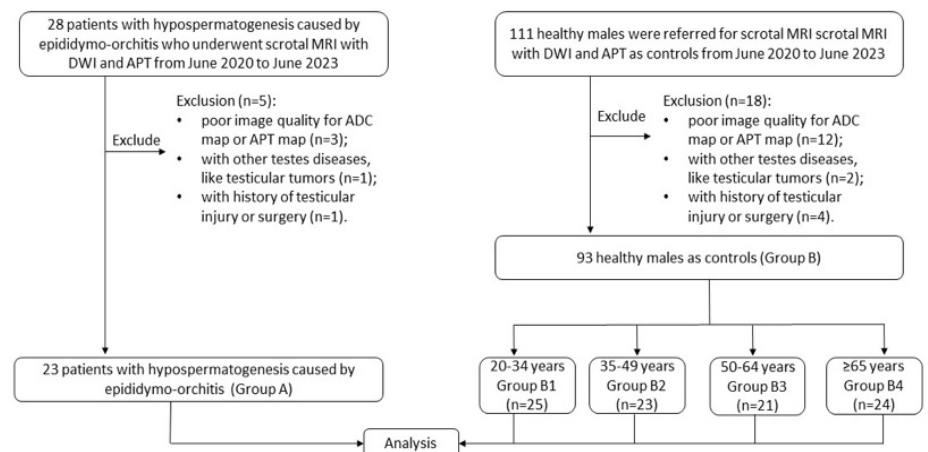


Figure 1. Study flowchart showing the patient inclusion and exclusion criteria. DWI, diffusion-weighted imaging; APT, amide proton transfer; MRI, magnetic resonance imaging; ADC, apparent diffusion coefficient.

2; and total scan time, 4 minutes and 59 seconds for each APTw scan.

Image analysis

The ADC and APT SI were independently measured by two radiologists (P.Y. and J.G., with 6 and 20 years of experience, respectively) blinded to clinical data, and average values were used. Circular regions of interest (ROIs) were placed centrally (with the center at the intersection of the long and short axes) on both the automatically generated ADC maps and the APTw maps to encompass most of the testes without artifacts or margins, with an area of no less than 110 mm². The ROIs are shown in Figure 2. Each testis was measured three times to determine the average ADC and APT SI.

Statistical analysis

Statistical analysis was performed using SPSS version 22 (IBM, Armonk, NY, USA). Data normality was assessed using the Shapiro-Wilk test. Continuous variables were expressed as mean ± standard deviation and categorical variables in terms of count. The ADC and APT SI values of the patients and the controls were compared using the independent samples t-test. Spearman's rank correlation coefficient was used to analyze correlations between age and APT/ADC.

Interobserver reproducibility was evaluated for ADC and APT SI measurements using the intraclass correlation coefficient (ICC). The level of agreement was considered excellent (ICC > 0.74), good (ICC = 0.60–0.74), fair (ICC = 0.40–0.59), or poor (ICC < 0.40). Statistical significance was defined as *P* < 0.05.

A priori power analysis was performed using G-Power software (version 3.1.9.7). To detect the difference in the APT SI and ADC value of testes between patients with epididymo-orchitis and the controls, a sample size of 15 was required for each group based on

these data. The sample size was considered sufficient to draw conclusions in this study.

Results

Average patient age and testicular APT SI and ADC values are listed in Table 1. In group B, Spearman's rank correlation coefficient showed that APT SI was negatively correlated with age (*r* = −0.510, *P* < 0.001) (Figure 3),

whereas ADC was positively correlated with age (*r* = 0.317, *P* = 0.006) (Figure 4). The APT SI was significantly higher in group A (1.77 ± 0.41) (Figure 3) compared with group B and all its subgroups (all *P* < 0.01). The ADC was significantly higher in group A [(0.549 ± 0.091) × 10^{−3} mm²/s] compared with group B [(0.482 ± 0.052) × 10^{−3} mm²/s, *P* < 0.001], including group B1 [(0.449 ± 0.047) × 10^{−3} mm²/s, *P* < 0.001], group B2 [(0.475 ± 0.022) ×

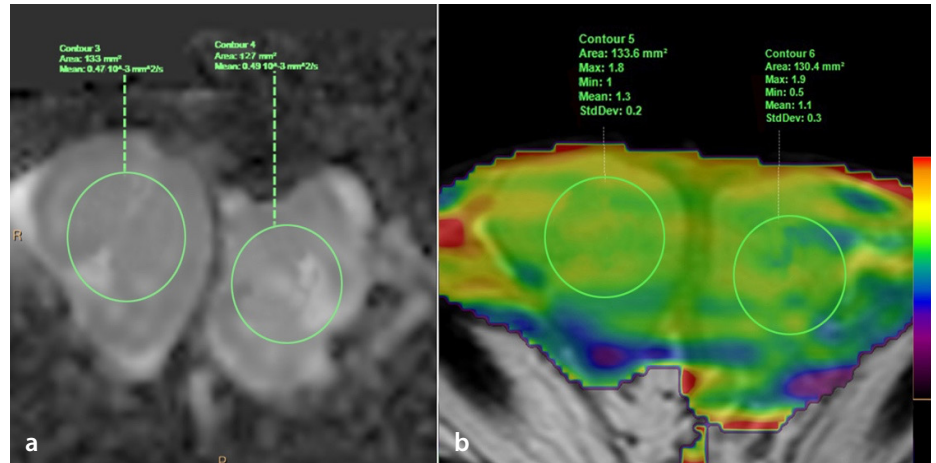


Figure 2. (a, b) Placement of regions of interest in testes.

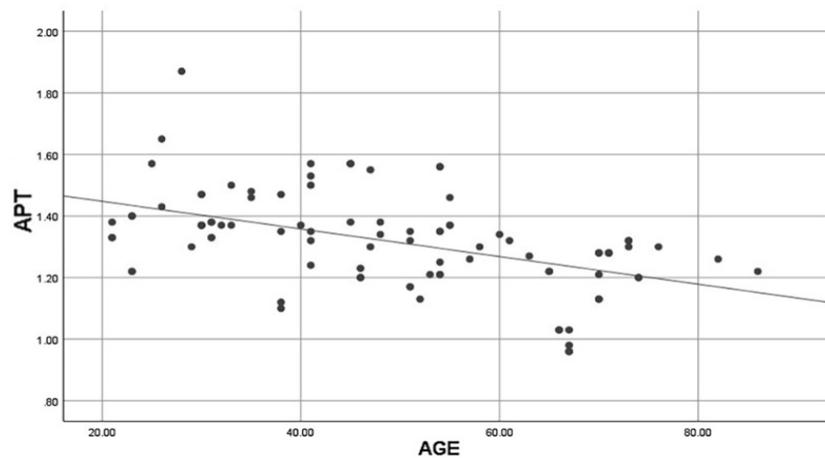


Figure 3. Scatter plot of APT signal intensity and age. APT, amide proton transfer.

Table 1. Testicular APT SI and ADC values in various groups

Group	Age	APT SI	<i>P</i> ^a	ADC (mm ² /s)	<i>P</i> ^b
Group A	36.40 ± 5.43	1.77 ± 0.29	NA	0.549 ± 0.091 × 10 ^{−3}	NA
Group B	48.97 ± 16.54	1.32 ± 0.16	<0.001	0.482 ± 0.052 × 10 ^{−3}	<0.001
Group B1	27.88 ± 3.85	1.43 ± 0.21	0.008	0.449 ± 0.047 × 10 ^{−3}	<0.001
Group B2	41.90 ± 4.15	1.37 ± 0.31	<0.001	0.475 ± 0.022 × 10 ^{−3}	0.002
Group B3	54.94 ± 3.70	1.30 ± 0.35	<0.001	0.488 ± 0.051 × 10 ^{−3}	<0.001
Group B4	71.50 ± 5.63	1.20 ± 0.35	<0.001	0.512 ± 0.089 × 10 ^{−3}	0.111

^a: Comparison with APT SI of group A. ^b: Comparison with ADC value of group A. APT SI, amide proton transfer signal intensity; ADC, apparent diffusion coefficient.

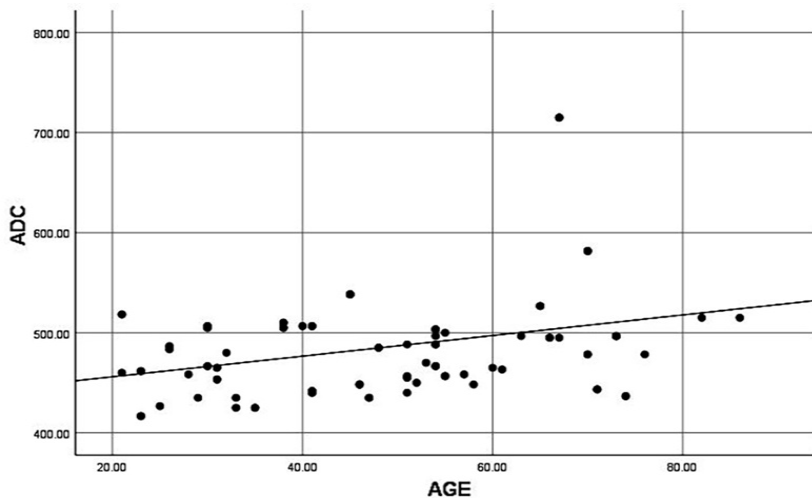


Figure 4. Scatter plot of ADC and age. ADC, apparent diffusion coefficient.

$10^{-3} \text{ mm}^2/\text{s}$, $P = 0.002$], and group B3 [$(0.488 \pm 0.051) \times 10^{-3} \text{ mm}^2/\text{s}$, $P < 0.001$], but there was no statistically significant difference between group A and group B4 [$(0.549 \pm 0.091) \times 10^{-3}$ vs. $(0.512 \pm 0.089) \times 10^{-3} \text{ mm}^2/\text{s}$, $P = 0.111$]. Examples of control groups and patients with epididymo-orchitis are shown in Figure 5.

Interobserver agreement was high for both the ADC (ICC = 0.850, 95% confidence interval (CI): 0.829–0.975) and the APT SI (ICC = 0.820, 95% CI: 0.805–0.853) measurements.

Discussion

Recently published studies have investigated the potential of functional MRI in male infertility.^{13,16,21} Proton MRS (^1H MRS), DWI, and MTI are promising for the evaluation of male infertility.^{13,16,21} Increased testicular ADC and decreased magnetization transfer ratio have been reported in patients with impaired spermatogenic function.^{13–15} Previous studies also reported that ^1H -MRS may be utilized for the evaluation of the testes of patients with NOA, in which decreased levels of choline, myoinositol, and lipids are found.^{20,21} Both ADC and MTI reflect certain histological features of testes, but neither can provide information at the levels of molecules and metabolites. Although ^1H -MRS may be valuable as a tool for quantitative evaluation of metabolites in spermatogenesis, the study of testes has adopted a common approach from brain MRS, which neglects the differences in metabolites between testes and the brain,^{20,21} meaning it is unclear whether the method can accurately reflect the actual metabolic status of the testis. Moreover,

APT_w imaging represents a non-invasive imaging technique, one used as an adjunct tool to conventional MRI that allows for the determination of metabolite concentration changes, such as mobile proteins and peptides in organs or tumors, and is utilized in studies involving brain tumors, hepatocellular carcinoma, bladder cancer, prostate cancer, and endometrioid endometrial adenocarcinoma.^{24–28} Beyond its applications in oncology, APT imaging has also been utilized in non-neoplastic conditions such as renal impairment^{35–36} and multiple sclerosis (MS).³⁷ In these studies, the potential mechanism underlying APT SI is hypothesized to be the increased concentration of mobile proteins and peptides during the progress of chronic kidney disease and within MS-associated chronic inflammatory lesions. Additionally, renal dysfunction will affect ion exchange and disrupt the original acid-base balance. This might change the pH value within tissue to a certain extent, leading to the increase of exchange rate between amide and water protons, consequently elevating the APT values. The concentration changes of a variety of proteins and peptides are involved in the production of spermatozoa by the testes,^{38,39} meaning applying APT in the evaluation of spermatogenic function of the testis is a promising approach. To the best of our knowledge, this is the first study that reports APT SI for the testis and spermatogenic function.

In this study, a negative correlation was found (coefficient: -0.510) between the APT SI of the testis and age in 94 healthy controls. In addition, the ADC value of normal testes increased with age, corroborating the find-

ings obtained by Wang et al.¹³ Aging in men is associated with both functional and structural alterations of the testis. With increasing age, testosterone levels and sperm production progressively decrease.^{5,6,40,41} Circulating testosterone levels are known to decrease by 0.4%–2% each year after the age of 30, which is due to altered Leydig cell number and function.^{4–6} In addition, the function of tubules and the number of Sertoli cells also decrease with age.^{5,6} According to previous reports, the APT SI of brain tumors is positively correlated with cellular density and/or proliferation (i.e., intracellular mobile protein and peptide concentrations).^{24,25} Therefore, decreased number of germ cells and reduced amounts of extracellular mobile proteins and peptides might account for APT SI reduction and ADC increase in testes. As such, elderly men with decreased spermatogenic function should, in theory, exhibit decreased APT and elevated ADC. The above results corroborate those of previous studies.^{13,14}

The testicular ADC values were higher in the patients with hypospermatogenesis caused by epididymo-orchitis (group A) than in all age groups of controls, including the oldest (group B4), which appeared to reflect impaired spermatogenic function in the group A patients. Moreover, the testicular APT SI values were significantly increased in group A compared with all age groups of controls, including the youngest (group B1). The results revealed that both ADC and APT could serve as biomarkers of impaired spermatogenic function caused by epididymo-orchitis. Interestingly, APT SI and ADC values in group A showed opposite trends of changes versus the observed trends with aging. Both parameters are believed to be related to cellular density,^{24,25,42,43} meaning reduced APT SI and elevated ADC should be observed in patients with hypospermatogenesis because of reduced cellular density. The abnormally elevated testicular APT SI in patients with epididymo-orchitis may be caused by the destruction of testes by active inflammation, which induces a series of pathological alterations, including microscopic necrosis, and an accumulation of testicular metabolites rich in mobile proteins and peptides. In addition, the APT SI is influenced by the chemical exchange rate between amide and water protons; this exchange rate depends mainly on the concentration of amide protons and the pH value in tissue.²³ We hypothesize that inflammatory reaction may alter the intracellular environment of testicular cells, thereby disrupting the original acid-base balance and changing the pH value in the testis to

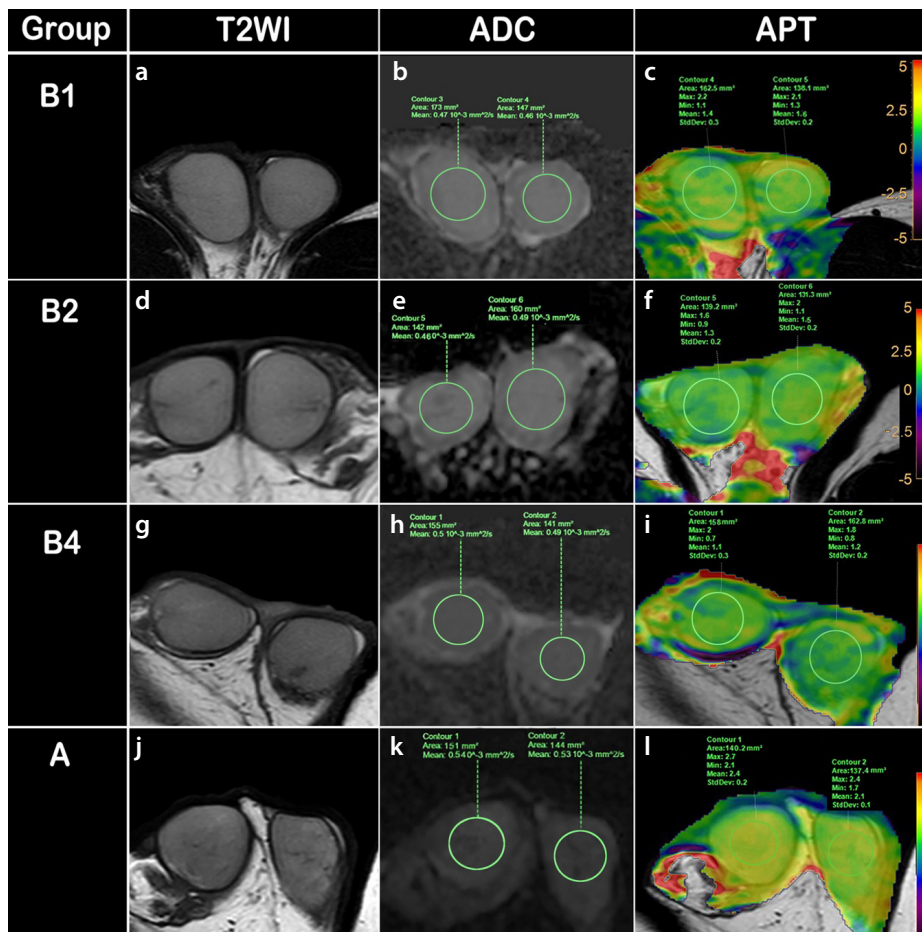


Figure 5. (a-c) A 25-year-old man in group B1 with normal semen analysis. (a) Axial T2-weighted imaging (WI) showing homogeneous hyperintensity of both testes. (b) An ADC map demonstrating average ADC values of $0.457 \times 10^{-3} \text{ mm}^2/\text{s}$ and $0.460 \times 10^{-3} \text{ mm}^2/\text{s}$ for the right and left testes, respectively. (c) Amide proton transfer (APT) map demonstrating low average APT signal intensity (SI) values of 1.5 and 1.45 for the right and left testes, respectively. (d-f) A 38-year-old man in group B2 with normal semen analysis. (d) Axial T2WI showing homogeneous hyperintensity of both testes. (e) ADC map demonstrating average ADC values of $0.460 \times 10^{-3} \text{ mm}^2/\text{s}$ and $0.490 \times 10^{-3} \text{ mm}^2/\text{s}$ for the right and left testes, respectively. (f) APT map demonstrating low average APT SI values of 1.3 and 1.5 for the right and left testes, respectively. (g-i) A 75-year-old man in group B4 married with two children, without traumatic history in testes. (g) Axial T2WI showing homogeneous hyperintensity of both testes. (h) ADC map demonstrating average ADC values of $0.510 \times 10^{-3} \text{ mm}^2/\text{s}$ and $0.490 \times 10^{-3} \text{ mm}^2/\text{s}$ for the right and left testes, respectively. (i) APT map demonstrating low average APT SI values of 1.1 and 1.2 for the right and left testes, respectively. (j-l) A 28-year-old man in group A with hypospermatogenesis caused by epididymo-orchitis who was clinically confirmed. (j) Axial T2WI showing homogeneous hyperintensity of both testes. (k) ADC map demonstrating higher average ADC values of $0.540 \times 10^{-3} \text{ mm}^2/\text{s}$ and $0.530 \times 10^{-3} \text{ mm}^2/\text{s}$ for the right and left testes, respectively, compared with controls. (l) Higher APT SI values of the right and left testes determined on the APT map (2.4 and 2.1, respectively) compared with controls.

a certain extent. This might accelerate the exchange rate between amide and water protons, leading to increased APT values. Further investigation is required to explore the mechanism underlying the changes of testicular APT SI in patients with epididymo-orchitis. The different trends of changes in APT SI and ADC may help determine the cause of hypospermatogenesis. A decreased APT SI combined with an increased ADC may suggest hypospermatogenesis caused by aging or chronic injuries, whereas an in-

creased APT SI combined with an elevated ADC is more likely to be associated with active or persistent inflammation. This may further improve clinical decision-making.

The limitations of this study are as follows. First, only a portion of the included volunteers (20–50 years old) underwent semen analysis to examine spermatogenic function. In addition, for volunteers over 50 years old, their statements of prior paternity were accepted as evidence of fertility, which might have led to errors in these age groups. Sec-

ond, generally no histopathologic confirmation was available for patients with suspected epididymo-orchitis, with all group A patients clinically confirmed by seminal plasma biochemistry. Third, the failure rate (23/139) of APTw imaging due to artifacts was still considerable and needs to be improved in the future. Finally, the heterogeneity in the severity distribution of hypospermatogenesis within our cohort (predominantly comprising severe cases), limits the generalizability of findings to milder forms of hypospermatogenesis. Future multicenter studies with larger, balanced samples are warranted to validate our findings.

In conclusion, according to the above preliminary results, the APT SI of normal testes tended to decrease with increasing age, whereas patients with hypospermatogenesis caused by epididymo-orchitis exhibited much higher APT SI compared with all age groups of controls. Thus, when combined with the ADC, which generally increases with both age and impaired spermatogenic function, APT SI may provide additional diagnostic information.

Footnotes

Funding

The work was supported by: (1) Science and Technology Projects in Guangzhou (number: SL2022A04J01837); (2) Medical Scientific Research Foundation of Guangdong Province, China (number: A2022008); (3) Natural Science Foundation of Tibet [number: XZZR202402135(W)].

Acknowledgments

We thank Mr. Jinhui Zhao and Ms. Jiaxui He (Department of Radiology, Linzhi People's Hospital, Tibet, PR China), for their support during this research.

Conflict of interest disclosure

The authors declared no conflicts of interest.

References

1. Theas MS. Germ cell apoptosis and survival in testicular inflammation. *Andrologia*. 2018;50(11):e13083. [Crossref]
2. Jalal H, Bahadur G, Knowles W, Jin L, Brink N. Mumps epididymo-orchitis with prolonged detection of virus in semen and the development of anti-sperm antibodies. *J Med Virol*. 2004;73(1):147-150. [Crossref]
3. Peng Y, Ouyang L, Lin Z, Zhang F, Wang H, Guan J. MRI findings of nonobstructive

- azoospermia: lesions in and out of pelvic cavity. *Abdom Radiol (NY)*. 2020;45(7):2213-2224. [\[Crossref\]](#)
4. Vermeulen A. Andropause. *Maturitas*. 2000;34(1):5-15. [\[Crossref\]](#)
 5. Kothari LK, Gupta AS. Effect of ageing on the volume, structure and total Leydig cell content of the human testis. *Int J Fertil*. 1974;19(3):140-146. [\[Crossref\]](#)
 6. Johnson L, Petty CS, Neaves WB. Influence of age on sperm production and testicular weights in men. *J Reprod Fertil*. 1984;70(1):211-218. [\[Crossref\]](#)
 7. Tsili AC, Giannakis D, Sylakos A, Ntorkou A, Sofikitis N, Argyropoulou MI. MR imaging of scrotum. *Magn Reson Imaging Clin N Am*. 2014;22(2):217-238, vi. [\[Crossref\]](#)
 8. Woldrich JM, Im RD, Hughes-Cassidy FM, Aganovic L, Sakamoto K. Magnetic resonance imaging for intratesticular and extratesticular scrotal lesions. *Can J Urol*. 2013;20(4):6855-6859. [\[Crossref\]](#)
 9. Tsili AC, Argyropoulou MI, Astrakas LG, et al. Dynamic contrast-enhanced subtraction MRI for characterizing intratesticular mass lesions. *AJR Am J Roentgenol*. 2013;200(3):578-585. [\[Crossref\]](#)
 10. Manganaro L, Saldari M, Pozza C, et al. Dynamic contrast-enhanced and diffusion-weighted MR imaging in the characterisation of small, non-palpable solid testicular tumours. *Eur Radiol*. 2018;28(2):554-564. [\[Crossref\]](#)
 11. Tsili AC, Argyropoulou MI, Giannakis D, Tsampalas S, Sofikitis N, Tsampoulas K. Diffusion-weighted MR imaging of normal and abnormal scrotum: preliminary results. *Asian J Androl*. 2012;14(4):649-654. [\[Crossref\]](#)
 12. Maki D, Watanabe Y, Nagayama M, et al. Diffusion-weighted magnetic resonance imaging in the detection of testicular torsion: feasibility study. *J Magn Reson Imaging*. 2011;34(5):1137-1142. [\[Crossref\]](#)
 13. Wang H, Guan J, Lin J, et al. Diffusion-weighted and magnetization transfer imaging in testicular spermatogenic function evaluation: preliminary results. *J Magn Reson Imaging*. 2018;47(1):186-190. [\[Crossref\]](#)
 14. Tsili AC, Astrakas LG, Goussia AC, Sofikitis N, Argyropoulou MI. Volumetric apparent diffusion coefficient histogram analysis of the testes in nonobstructive azoospermia: a noninvasive fingerprint of impaired spermatogenesis? *Eur Radiol*. 2022;32(11):7522-7531. [\[Crossref\]](#)
 15. Han BH, Park SB, Seo JT, Chun YK. Usefulness of testicular volume, apparent diffusion coefficient, and normalized apparent diffusion coefficient in the MRI evaluation of infertile men with azoospermia. *AJR Am J Roentgenol*. 2018;210(3):543-548. [\[Crossref\]](#)
 16. Tsili AC, Ntorkou A, Goussia A, et al. Diffusion tensor imaging parameters in testes with nonobstructive azoospermia. *J Magn Reson Imaging*. 2018;48(5):1318-1325. [\[Crossref\]](#)
 17. Tsili AC, Ntorkou A, Baltogiannis D, et al. Magnetization transfer imaging of normal and abnormal testis: preliminary results. *Eur Radiol*. 2016;26(3):613-621. [\[Crossref\]](#)
 18. Ntorkou A, Tsili AC, Goussia A, et al. Testicular apparent diffusion coefficient and magnetization transfer ratio: can these MRI parameters be used to predict successful sperm retrieval in nonobstructive azoospermia? *AJR Am J Roentgenol*. 2019;213(3):610-618. [\[Crossref\]](#)
 19. Firat AK, Uğraş M, Karakaş HM, et al. 1H magnetic resonance spectroscopy of the normal testis: preliminary findings. *Magn Reson Imaging*. 2008;26(2):215-220. [\[Crossref\]](#)
 20. Aaronson DS, Iman R, Walsh TJ, Kurhanewicz J, Turek PJ. A novel application of 1H magnetic resonance spectroscopy: non-invasive identification of spermatogenesis in men with non-obstructive azoospermia. *Hum Reprod*. 2010;25(4):847-852. [\[Crossref\]](#)
 21. Ntorkou A, Tsili AC, Astrakas L, et al. In vivo biochemical investigation of spermatogenic status: 1H-MR spectroscopy of testes with nonobstructive azoospermia. *Eur Radiol*. 2020;30(8):4284-4294. [\[Crossref\]](#)
 22. Zhou J, Lal B, Wilson DA, Lartera J, van Zijl PC. Amide proton transfer (APT) contrast for imaging of brain tumors. *Magn Reson Med*. 2003;50(6):1120-1126. [\[Crossref\]](#)
 23. Zhou J, Payen JF, Wilson DA, Traustman RJ, van Zijl PC. Using the amide proton signals of intracellular proteins and peptides to detect pH effects in MRI. *Nat Med*. 2003;9(8):1085-1090. [\[Crossref\]](#)
 24. Togao O, Yoshiura T, Keupp J, et al. Amide proton transfer imaging of adult diffuse gliomas: correlation with histopathological grades. *Neuro-oncology*. 2014;16(3):441-448. [\[Crossref\]](#)
 25. Zhou J, Blakeley JO, Hua J, et al. Practical data acquisition method for human brain tumor amide proton transfer (APT) imaging. *Magn Reson Med*. 2008;60(4):842-849. [\[Crossref\]](#)
 26. Wang HJ, Cai Q, Huang YP, et al. Amide proton transfer-weighted MRI in predicting histologic grade of bladder cancer. *Radiology*. 2022;305(1):E59. [\[Crossref\]](#)
 27. Takayama Y, Nishie A, Sugimoto M, et al. Amide proton transfer (APT) magnetic resonance imaging of prostate cancer: comparison with Gleason scores. *Magma*. 2016;29(4):671-679. [\[Crossref\]](#)
 28. Takayama Y, Nishie A, Togao O, et al. Amide proton transfer MR imaging of endometrioid endometrial adenocarcinoma: association with histologic grade. *Radiology*. 2018;286(3):909-917. [\[Crossref\]](#)
 29. Li C, Peng S, Wang R, et al. Chemical exchange saturation transfer MR imaging of Parkinson's disease at 3 Tesla. *Eur Radiol*. 2014;24(10):2631-2639. [\[Crossref\]](#)
 30. Björndahl L, Kirkman Brown J; other Editorial Board Members of the WHO Laboratory Manual for the Examination and Processing of Human Semen. The sixth edition of the WHO laboratory manual for the examination and processing of human semen: ensuring quality and standardization in basic examination of human ejaculates. *Fertil Steril*. 2022;117(2):246-251. [\[Crossref\]](#)
 31. Street EJ, Justice ED, Kopa Z, et al. The 2016 European guideline on the management of epididymo-orchitis. *Int J STD AIDS*. 2017;28(8):744-749. [\[Crossref\]](#)
 32. Kopa Z, Wenzel J, Papp GK, Haidl G. Role of granulocyte elastase and interleukin-6 in the diagnosis of male genital tract inflammation. *Andrologia*. 2005;37(5):188-194. [\[Crossref\]](#)
 33. Collodel G, Nerucci F, Signorini C, Iacoponi F, Moretti E. Associations between biochemical components of human semen with seminal conditions. *Syst Biol Reprod Med*. 2019;65(2):155-163. [\[Crossref\]](#)
 34. Zorn B, Sesek-Briski A, Osredkar J, Meden-Vrtovec H. Semen polymorphonuclear neutrophil leukocyte elastase as a diagnostic and prognostic marker of genital tract inflammation—a review. *Clin Chem Lab Med*. 2003;41(1):2-12. [\[Crossref\]](#)
 35. Ju Y, Wang Y, Luo RN, et al. Evaluation of renal function in chronic kidney disease (CKD) by mDIXON-quant and amide proton transfer weighted (APT_w) imaging. *Magn Reson Imaging*. 2023;103(9):102-108. [\[Crossref\]](#)
 36. Ju Y, Liu A, Wang Y, et al. Amide proton transfer magnetic resonance imaging to evaluate renal impairment in patients with chronic kidney disease. *Magn Reson Imaging*. 2022;87(3):177-182. [\[Crossref\]](#)
 37. By S, Barry RL, Smith AK, et al. Amide proton transfer CEST of the cervical spinal cord in multiple sclerosis patients at 3T. *Magn Reson Med*. 2018;79(2):806-814. [\[Crossref\]](#)
 38. Schlegel PN, Katzovitz MA. Male Reproductive Physiology. In: Chapple CR, Steers WD, Evans CP, editors. *Urologic Principles and Practice*. Cham: Springer International Publishing; 2020:41-62. [\[Crossref\]](#)
 39. Neto FT, Bach PV, Najari BB, Li PS, Goldstein M. Spermatogenesis in humans and its affecting factors. *Semin Cell Dev Biol*. 2016;59:10-26. [\[Crossref\]](#)
 40. Tajar A, Forti G, O'Neill TW, et al. Characteristics of secondary, primary, and compensated hypogonadism in aging men: evidence from the European male ageing study. *J Clin Endocrinol Metab*. 2010;95(4):1810-1818. [\[Crossref\]](#)
 41. Araujo AB, O'Donnell AB, Brambilla DJ, et al. Prevalence and incidence of androgen deficiency in middle-aged and older

- men: estimates from the Massachusetts male aging study. *J Clin Endocrinol Metab.* 2004;89(12):5920-5926. [\[Crossref\]](#)
42. Mazaheri Y, Shukla-Dave A, Hricak H, et al. Prostate cancer: identification with combined diffusion-weighted MR imaging and 3D 1H MR spectroscopic imaging--correlation with pathologic findings. *Radiology.* 2008;246(2):480-488. [\[Crossref\]](#)
43. Zelhof B, Pickles M, Liney G, et al. Correlation of diffusion-weighted magnetic resonance data with cellularity in prostate cancer. *BJU Int.* 2009;103(7):883-888. [\[Crossref\]](#)